Article:

Li, Z, Jiu, L, Gong, Y. et al. (4 more authors) (2017) Semi-polar (11-22) AlGaN on overgrown GaN on micro-rod templates: Simultaneous management of crystal quality improvement and cracking issue. Applied Physics Letters, 110 (8). ISSN 0003-6951

https://doi.org/10.1063/1.4977094

Semi-polar (11-22) AlGaN on overgrown GaN on micro-rod templates: simultaneous management of crystal quality improvement and cracking issue

Z. Li, L. Jiu, Y. Gong, L. Wang, Y. Zhang, J. Bai and T. Wang*

Department of Electronic and Electrical Engineering, University of Sheffield, Mappin Street, Sheffield, S1 3JD, United Kingdom

Abstract

Thick and crack-free semi-polar (11-22) AlGaN layers with various high Al composition have been achieved by means of growth on the top of nearly but not yet fully-coalesced GaN overgrown on micro-rod templates. The Al composition achieved has a range of up to 55.7%, corresponding an emission wavelength of up to 270 nm characterised by photoluminescence at room temperature. X-ray diffraction (XRD) measurements show greatly improved crystal quality as a result of lateral overgrowth compared to the AlGaN counterparts on standard planar substrates. The full width at half maximums (FWHM) of the XRD rocking curves measured along the [1-100]/[11-2-3] directions (the two typical orientations for characterizing the crystal quality of (11-22) AlGaN) are $0.2923^0/0.2006^0$ for 37.8% Al and $0.3825^0/0.2064^0$ for 55.7% Al, respectively, which have never been achieved previously. Our calculation based on reciprocal space mapping measurements has demonstrated significant strain relaxation in the AlGaN as a result of utilising the non-coalesced GaN underneath, contributing to the elimination of any cracks. The results presented have demonstrated that our overgrowth technique can effectively manage strain and improve crystal quality simultaneously.

PACS Number: 68.37.Lp, 81.15.Gh, 68.55.Jk, 68.37.Ps

---

[*] Authors to whom correspondence should be addressed, electronic mail: t.wang@sheffield.ac.uk

There is an increasing demand in developing ultra-violet (UV) emitters, in particular deep UV emitters for wide applications in water purification, environmental protection, medical instrumentation, non-line-of-sight communications, etc, where AlGaN with high Al composition is a promising semiconductor candidate.[1] So far, the studies on AlGaN based UV emitters are mainly limited to polar-oriented AlGaN grown on *c-plane* sapphire, where their active regions suffer from polarization induced electrical fields leading to a reduction in optical efficiency, namely, quantum-confined stark effect (QCSE). Furthermore, AlGaN grown on GaN suffers from tensile strain, leading to extensive cracks often observed on *c-plane* AlGaN. Both the QCSE and the cracking issue become more severe with further increasing Al composition for deep UV emitters. The growth of AlGaN layers along a semi-/non-polar direction is a promising solution, which can minimize or eliminate the QCSE and hence improve optical efficiency. However, the great challenge is due to the crystal quality of semi-polar AlGaN which is far from satisfactory.

Previously a number of methods were developed in order to obtain high quality AlGaN grown on *c-plane* sapphire, such as migration-enhanced metalorganic chemical vapor deposition (MOCVD) [2] and ammonia pulsed-flow multilayer growth technique.[3] A number of approaches have also been proposed in order to manage the strain of thick AlGaN films grown on *c-plane* substrates, such as using interlayers [4] or superlattice layers.[5] However, so far there are only a few reports on improving the crystal quality and addressing the cracking issue in semi-polar AlGaN.[6-8] Balakrishnan et al.[6-7] obtained thick and crack-free n-AlGaN (11-22) films by inserting a strain relieving AlN/AlGaN short-period superlattice structure on sapphire. Young et al.[8] reported the compositionally graded semi-polar AlGaN epilayers on expensive freestanding semi-polar (20-21) GaN substrates.

So far, it is a great challenge to achieve thick and crack-free semi-polar AlGaN with high crystal quality on cost-effective sapphire. Previously, our group developed a different overgrowth approach of semi-polar (11-22) GaN on micro-rod arrayed templates, leading to significantly improved crystal quality of semi-polar (11-22) GaN on sapphire.[9-11]

In this paper, we have achieved thick and crack-free semi-polar (11-22) AlGaN layers with various high Al compositions grown on nearly but not yet fully-coalesced GaN overgrown on micro-rod templates, managing both cracking issues and quality improvement simultaneously. The non-coalesced GaN layer underneath is specially designed in order to effectively relax the strain which the overlying AlGaN suffers. The AlGaN layers have been found to be compressively strained instead of being conventionally tensilely strained, preventing cracks. The crystal quality of AlGaN is significantly improved via the overgrowth approach compared with any conventional AlGaN counterparts on planar substrates.

Fig. 1a schematically illustrates our fabrication and growth procedure for semi-polar AlGaN. A 400 nm (11-22) GaN layer was grown on *m-plane* sapphire using our high temperature (HT) AlN buffer technique [12] by MOCVD. The as-grown GaN template was then etched into micro-rod arrays using a standard photolithography technique and subsequent dry-etching processes.[9-11] Subsequently, the micro-rod array template with SiO_2 on the top of each rod was reloaded for further overgrowth of GaN and AlGaN. An initial overgrowth of GaN was carried out for 3000s, allowing the overgrown semi-polar GaN to be nearly but not yet fully-coalesced. Thick AlGaN layers with Al composition ranging from 37.8% to 55.7% in each sample was then grown on the non-coalesced GaN. *All the samples were grown at 1145^{0}C using a V/III ratio of ~800 under 65 torr, but with a systematic change in the flow-rate ratio of trimethylaluminium (TMAl) to trimethylgallium (TMGa) from 2 to 5.9.*

Crystal quality of the AlGaN epilayers is characterized by X-ray diffraction (XRD) measured in a ω/2θ scanning mode and further evaluated by azimuth-dependent XRD rocking curve measurements. Photoluminescence (PL) measurements have been performed at room temperature (RT) by using a doubled-frequency Argon ion laser at 244 nm. In order to study the strain of the semi-polar AlGaN as a function of Al composition, multiple on- and off-axis XRD measurements have been conducted. Reciprocal space mapping (RSM) has been further measured along both the [1-100] and the [11-2-3] in-plane directions to analyse the strain in detail.

Fig. 1b shows a typical scanning electron microscopy (SEM) cross-sectional image of our overgrown AlGaN, where the semi-polar GaN below the AlGaN layer is nearly but not yet fully-coalesced. The thicknesses of the GaN and the AlGaN are ~2.7 and ~2.1 µm, respectively. Triangular residual voids with a feature size of ~1 µm are formed at the micro-rod spacing during the first GaN coalescence process and on the top of rods during the second GaN coalescence process. The details of the overgrown GaN can be found elsewhere.[9-11] The AlGaN growth initiated just before the second coalescence process was fully completed, resulting in the non-coalesced GaN and the residual voids underneath, as denoted by a circle in **Fig. 1b**, where as an example the inset shows a typical SEM top-view image of the AlGaN, exhibiting a smooth and crack-free surface with stripe-like features along the [11-2-3] direction. Such stripe features are typical for a semi-polar sample and become more prominent when the Al composition increases. It is worth highlighting that all the AlGaN samples don't have any cracks across a 2-inch wafer. It is well-known that AlGaN directly grown on planar GaN suffers from tensile strain. The critical thickness of (11-22) AlGaN on GaN is only several tens of nanometres for 20% Al composition and then decreases with higher Al composition (<10nm for 40% Al content).[13] Serious wafer cracking has been often observed when semi-polar (11-22) AlGaN is directly grown on planar GaN. The crack-free features in our high Al composition AlGaN samples suggest a remarkably different strain status via our developed overgrowth technique.

Fig. 2a shows the XRD data measured in a ω/2θ mode on all the samples. The diffraction peaks from (30-30) sapphire, (11-22) GaN and AlGaN have been clearly observed, with the former two peaks remaining unchanged when the Al composition varies. *The Al composition ranges from 37.8% to 55.7%. In each sample, the Al content is determined based on the XRD diffraction angle of the*

AlGaN layer using the XRD diffraction angle of either sapphire or the GaN as a reference. **Fig. 2b** shows the RT PL spectra, demonstrating the emission wavelength ranges from 309 to 270 nm when the Al composition increases from 37.8% to 55.7%. Moreover, the PL spectra exhibit a single peak for the samples with Al composition below 45%, whereas a shoulder peak appears on the long wavelength side when the Al composition is higher than 45%. Our cathodoluminescence measurements[14] show that the regions directly on the top of the SiO_2 mask regions for the samples with high Al composition show slightly lower Al composition than that in the window regions between the masks, possibly resulting in the shoulder peaks on the longer wavelength side.

XRD rocking curves have been measured as a function of azimuth angle from 0^0 to 180^0. As an example, **Fig. 3a** provides the full width at half maximums (FWHM) of the XRD rocking curves measured on the sample with 37.8% Al, showing a typical behaviour for a semi-polar sample, namely, the lowest FWHM along [11-2-3] (i.e., 90^0 azimuth angle) and the largest FWHM along [1-100] (i.e., zero azimuth angle). For comparison, the FWHMs of the underlying non-coalesced GaN, an as-grown (11-22) GaN (used for the fabrication of a micro-rod template), and a standard (11-22) AlGaN (non-overgrown) with similar Al composition of 37% are also presented. Compared with the as-grown GaN, the crystal quality of the non-coalesced GaN is greatly improved as a result of the effective blockage of the defects due to overgrowth.[9] The overgrown GaN (although non-coalesced) serves as a good template for the subsequent AlGaN growth, thus leading to the further overgrown AlGaN with improved crystal quality. Compared with the standard (11-22) AlGaN sample with a similar thickness and Al composition obtained using our HT AlN buffer on *m-plane* sapphire,[12] the crystal quality of our overgrown AlGaN has been significantly improved, confirmed by the XRD rocking curve FWHMs of 0.2923^0 along [1-100] and 0.2006^0 along [11-2-3]. In contrast, the standard AlGaN exhibits the FWHMs of 0.5020^0 along [1-100] and 0.3047^0 along [11-2-3]. *Note that Strain relaxation has been studied on the standard semi-polar AlGaN grown on the AlN buffer along two typical orientations (i.e., (1-100) and (11-2-3)), showing that the AlGaN* *layer suffers from compressive strain along both orientations. The strain status of the AlGaN on the AlN buffer, in particular along the (1-100) orientation, is very similar to c-plane AlGaN grown on an AlN buffer.* [15]

Fig. 3b presents the FWHMs of the XRD rocking curves of our semi-polar AlGaN samples as a function of Al composition, indicating that the FWHMs along the [1-100]/[11-2-3] directions increases from $0.2923^{0}/0.2006^{0}$ to $0.3865^{0}/0.2064^{0}$ for the AlGaN with Al composition increasing from 37.8 to 55.7%. *These represent the lowest values reported for the (11-22) AlGaN with similar Al composition.*[6,16,17] *It means that our samples (although grown under un-optimized conditions) demonstrate a step-change in crystal quality which has not been achieved previously*.

Note that all semi-polar GaN and AlGaN samples exhibit anisotropic broadening in XRD rocking curves: FWHM along [1-100] is broader than that along [11-2-3]. Such anisotropic property has been widely reported in semi- or non- polar structures.[17,18] It has been suggested that either mosaic tilt of epilayers or basal stacking faults (BSFs) could cause anisotropic broadening.[19] Here, in order to analyse the in-plane anisotropy of crystal quality, we define an anisotropy degree as

$$\rho = (\mathrm{FWHM}_{1\text{-}100} - \mathrm{FWHM}_{11\text{-}2\text{-}3}) / (\mathrm{FWHM}_{1\text{-}100} + \mathrm{FWHM}_{11\text{-}2\text{-}3})$$

where $\mathrm{FWHM}_{1\text{-}100}$ and $\mathrm{FWHM}_{11\text{-}2\text{-}3}$ corresponds to the values measured along the [1-200] and the [11-2-3] directions, respectively. **Fig. 3c** shows the anisotropy degree as a function of Al composition. An anisotropy degree can also be affected by crystal quality. For an instance, the XRD anisotropy of high-quality overgrown GaN is almost smeared out leading to ρ=0.02, whereas standard semi-polar GaN without using any overgrowth technique exhibits a strong anisotropic feature, typically ρ=0.33. Similarly, the overgrown AlGaN (ρ=0.17, for 37.8% Al) also shows weaker anisotropic features than the standard AlGaN (ρ=0.25, with 37% Al).

Our PL measurements (not shown) at 10K show that the intensity ratio of the AlGaN near band emission (NBE) to its BSF related emission is typically ~30% for the standard AlGaN and ~2.5% for the as-grown GaN, while ~90% for our overgrown AlGaN and ~800% for our overgrown GaN.[9] These also confirm a significant reduction in BSF density for our overgrown samples. One can assume that BSFs are the predominating source for the strong anisotropic broadening of the XRD rocking curves.[19] On the other hand, it can be observed in **Fig. 3c**, the anisotropy degree is around 0.2 (the left circle) for the overgrown AlGaN samples with low Al composition below from 0.40, while the anisotropy degree remains around 0.33 for higher Al composition samples (the right circle). Since the BSF densities in all the overgrown AlGaN samples are actually comparable, confirmed by the NBE/BSF PL intensity ratios measured at 10K (all around 90~110%), the enhanced anisotropy degree as a result of increasing Al composition could be mainly attributed to the lattice tilt, which is in turn due to an increase in lattice mismatch between AlGaN and GaN.

Unlike the strain in c-plane AlGaN/GaN, it becomes complicated in semi-polar structures due to reduced symmetry and more complex distortion. Based on a triclinic unit cell mode, Frentrup et al.[20] have developed an approach to determining the lattice parameters of semi-polar (11-22) structures using multiple on- and off-axis XRD measurement in a ω/2θ mode. The interplanar spacing d_{hkl} of {hkil} planes is expressed by lattice parameters (a, c, α, γ) as

$$\frac{1}{d_{hkl}^2}=\frac{4}{3}\frac{(h^2+k^2+l^2)}{a^2}+\frac{l^2}{c^2}+\frac{(8h^2+8k^2+20hk)}{3\sqrt{3}a^2}\delta_\gamma+\frac{4(hl+kl)}{ac}\delta_\alpha \qquad (1)$$

where δ_α and δ_γ are the offset of basis angles α and γ, respectively, showing the distortion and shearing of a semi-polar unit cell.[20] Based on the above equation, the lattice parameters of our overgrown AlGaN can be extracted. Below is an example using the overgrown AlGaN with Al composition of 39.9%. A series of multiple on- and off-axis XRD measurements for the overgrown AlGaN and the GaN underneath have been carried out, respectively, namely, (0002), (0004), (11-20), (2-1-12), (-12-1-2), (11-22), (11-24), (1-103) and (1-101). Based on equation 1, their lattice parameters have been obtained: a = (3.1743 ± 0.0001) Å, c = (5.1947 ± 0.0001) Å, α = (90.00^0±

0.02^0) and γ= (119.99^0± 0.01^0) for the underlying GaN; a = (3.1501 ± 0.0001) Å, c = (5.1091 ± 0.0001) Å, α = (89.99^0± 0.02^0) and γ= (119.99^0± 0.02^0) for the AlGaN. The basis angles α and γ in both layers are quite close to their respective counterparts in an unstrained state, indicating negligible distortion or shearing as a result of significant strain relaxation. With the lattice parameters derived above, the out-of-plane and in-plane strain in the AlGaN and the GaN layers can be then deduced from equations below:

$$\varepsilon_{11-22} = \frac{d_{11-22}^{meas} - d_{11-22}^{0}}{d_{11-22}^{0}}$$

$$\varepsilon_{11-2-3} = \frac{L_{11-2-3}^{meas} - L_{11-2-3}^{0}}{L_{11-2-3}^{0}} \quad \text{and} \quad \varepsilon_{1-100} = \frac{L_{1-100}^{meas} - L_{1-100}^{0}}{L_{1-100}^{0}}$$

where d and L are the interplanar spacing and distance, respectively; index “0” and “meas” denote the unstrained and strained layers, respectively. The calculated strains are summarized in Table I.

It has been found that both the AlGaN and the underlying GaN exhibit anisotropic in-plane compressive strains. For the underlying GaN, the in-plane strain along [11-2-3] is -5.8482×10^{-5}, approaching to zero and thus indicating almost complete relaxation along this direction, while the strain along [1-100] is two-order magnitude higher than that along [11-2-3], showing much higher compressive strain. This anisotropic strain in the overgrown GaN layer could be understood from the overgrowth process. The GaN overgrowth initiated from the sidewalls of micro-rods and advanced along the ***c*** and ***a*** direction, where the ***c***-growth is much faster than the ***a***-growth. The predominant ***c***-growth should lead to large strain relaxation along the [11-2-3] direction which is the in-plane projection of the ***c***-direction. The voids, formed when the ***c***-growth facet meets with the ***a***-growth facet, can effectively block the BSFs and cause either annihilation or termination of dislocations [9,21] along with the strain relaxation simultaneously. The second GaN coalescence which is not completely finished further maintains the strain relaxation of the GaN layer. Moreover, the anisotropic lattice mismatch between GaN and sapphire, which is 1% along the ***c***-

direction and 16% along the ***m**-direction,*[22] respectively, also probably contributes to the in-plane strain anisotropy.

For the AlGaN layer, it exhibits compressive instead of tensile strain. This is typical for semipolar AlGaN grown on GaN [20] which is different from *c-plane* AlGaN. The strain along the [1-100] is about three times larger than that along the [11-23] direction. Due to the non-coalesced GaN underneath, the AlGaN growth proceeds laterally at the initial stage. Similar to the GaN overgrowth, the lateral overgrowth along the ***c***-direction in the AlGaN also results in much larger strain relaxation than that along the [11-2-3] direction. Furthermore, the strain relaxation can effectively occur as a result of residual voids formed when the AlGaN was grown on the non-coalesced GaN. Therefore, the great improvement in the crystal quality of AlGaN is attributed not only to the high-quality GaN underneath, but also to the great strain relaxation providing less chance for the formation of dislocations or wafer cracking.

The strain has been further investigated by XRD reciprocal space mapping (RSM) measurements in which the distortion or relaxation of the reciprocal lattice point (RLP) can be clearly observed. As an example, **Fig. 4** shows the (11-22) RSM of the AlGaN with Al composition of 39.9%. When the (11-22) RSM is measured along [1-100], the RLPs of the GaN and the AlGaN nearly stand in a straight line with the RLP of sapphire, showing that the AlGaN is coherently grown on the GaN layers along this direction. However, along [11-2-3], the epitaxial tilt between the three layers can be clearly observed. A tilt angle of 0.50^0 is exhibited for the underlying GaN layer with respect to the *m-plane* sapphire while a tilt of 1.10^0 for the AlGaN layer with respect to the underlying GaN. This is in good agreement with the above analysis that $\varepsilon_{1\text{-}100}$ is much larger than $\varepsilon_{11\text{-}2\text{-}3}$ in both the GaN and the AlGaN. Tyagi et al.[23] have reported that lattice tilt could cause partial strain relaxation via misfit dislocation generation at the AlGaN/GaN interface and even be used to quantify the strain relaxation. In comparison with other reports, [8,24] the increased tilt angle in our AlGaN sample indicates enhanced strain relaxation, agreeing with the residue strain obtained above.

Crack-free and thick semi-polar (11-22) AlGaN with high Al composition of up to 55.7% (corresponding to a RT PL emission at 270nm) have been grown on our specially designed overgrown GaN. The FWHMs of the XRD rocking curves along the [1-100]/[11-2-3] directions are 0.2923^0/0.2006^0 for 37.8% Al and 0.3825^0/0.2064^0 for 55.7% Al, respectively, representing the best report for semi-polar AlGaN reported so far. The strain have been investigated by means of multiple on- and off-axis XRD measurements along with the (11-22) RSM measurements, showing compressive instead of tensile in-plane strain and also significant strain relaxation in our AlGaN layers. It indicates that our overgrowth method is an effective way to both release the strain and improve the crystal quality simultaneously, which plays an important role in developing semi-polar deep UV emitters with a step-change in optical performance.

Acknowledgements

Financial support is acknowledged from the EPSRC, UK via Grant No. EP/M003132/1

References

[1]A. Khan, K. Balakrishnan and T. Katona, *Nat. Photonics* 2 77 (2008).

[2]J. Zhang, X. Hu, A. Lunev, J. Deng, Y. Bilenko, T. M. Katona, M. S. Shur, R. Gaska and M. A. Khan, *Jpn. J. Appl. Phys.* 44 7250 (2011).

[3]H. Hirayama, T. Yatabe, N. Noguchi, T. Ohashi and N. Kamata, *Appl. Phys. Lett.* 91 071901 (2007).

[4]H. Amano, M. Iwaya, N. Hayashi, T. Kashima, S. Nitta, C. Wetzel and I. Akasaki, *Phys. Stat. Sol. B* 216 683 (1999).

[5]J. P. Zhang, H. M. Wang, M. E. Gaevski, C. Q. Chen, Q. Fareed, J. W. Yang, G. Simin and M. A. Khan, *Appl. Phys. Lett.* 80 3542 (2002).

[6]K. Balakrishnan, M. Lachab, H. C. Chen, D. Blom, V. Adivarahan, I. Ahmad, Q. Fareed and M. A. Khan, *Phys. Stat. Sol.* A 208 2724 (2011).

[7]K. Balakrishnan, V. Adivarahan, Q. Fareed, M. Lachab, B. Zhang and A. Khan, *Jpn J. Appl. Phys. Lett.* 49 040206 (2010).

[8]E. C. Young, F. Wu, A. E. Romanov, D. A. Haeger, S. Nakamura, S. P. Denbaars, D. A. Cohen and J. S. Speck, *Appl. Phys. Lett.* 101 142109 (2012).

[9]Y. Zhang, J. Bai, Y.Hou, R. M. Smith, X. Yu, Y. Gong and T. Wang, *AIP Advances* 6 025201 (2016).

[10]T. Wang, *Semicond. Sci. Technol.* 31 093003 (2016) (A topical Review and references therein)

[11]J. Bai, B. Xu, F. G. Guzman, K. Xing, Y. Gong, Y. Hou and T. Wang, *Appl. Phys. Lett.* 107 261103 (2015).

[12]T. Wang, J. Bai, P. J. Parbrook, and A. G. Cullis, *Appl. Phys. Lett.* 87 151906 (2005).

[13]E. C. Young, C. S. Gallinat, A. E. Romanov, A. Tyagi, F. Wu and J. S. Speck, *Appl. Phys. Express* 3 111002 (2010).

[14]Z. Li, L. Wang, L. Jiu, Y. Gong, Y. Zhang, J. Bruckbauer, J. Bai, R. Martin and T. Wang, unpublished.

[15] Y. Gong, K. Xing, and T. Wang, *Appl. Phys. Lett.* 99 171912 (2011).

[16]J. Stellmach, F. Mehnke, M. Frentrup, C. Reich, J. Schlegel, M. Pristovsek, T. Wernicke and M. Kneissl, *J. Cryst. Growth* 367 42 (2013).

[17]N. Hatui, A. A. Rahman, C. B. Maliakkal and A. Bhattacharya, *J. Cryst. Growth* 437 1 (2016).

[18]M. A. Moram, C. F. Johnston, J. L. Hollander, M. J. Kappersand C. J. Humphreys, *J. Appl. Phys.* 105 113501 (2009).

[19]M. B. Mclaurin, A. Hirai, E. Young, F. Wu, and J. S. Speck, *Jpn J. Appl. Phys.* 47 5429 (2008).

[20]M. Frentrup, N. Hatui, T. Wernicke, J. Stellmach, A. Bhattacharya, and M. Kneissl, *J. Appl. Phys.* 114 213509 (2013).

[21]J. Bai, Y. Gong, K. Xing, X. Yu and T. Wang, *Appl. Phys. Lett.*102 101906 (2013).

[22]M. Tsuda, H. Furukawa, A. Honshio, M. Iwaya, S. Kamiyama, H. Amano and I. Akasaki, *Phys. Stat. Sol.* B 243 1524 (2006).

[23]A. Tyagi, F. Wu, E. C. Young, A. Chakraborty, H. Ohta, R. Bhat, K. Fujito, S. P. Denbaars, S. Nakamura and J. S. Speck, *Appl. Phys. Lett.* 95 251905 (2009).

[24]D. V. Dinh, M. Conroy, V. Z. Zubialevich, N. Petkov, J. D. Holmes and P. J. Parbrook, *J. Cryst. Growth* 414 94 (2015).

Table I Calculated Strain in (11-22) GaN and AlGaN (39.9%Al)

Epilayers	In-plane strain		Out-of-plane strain
	$\varepsilon_{11\text{-}2\text{-}3}$	$\varepsilon_{1\text{-}100}$	$\varepsilon_{11\text{-}22}$
Overgrown GaN	-5.8482×10^{-5}	-4.7737×10^{-3}	$+1.1651 \times 10^{-3}$
AlGaN	-1.1895×10^{-3}	-3.3888×10^{-3}	$+1.6665 \times 10^{-3}$

'+' means tensility; '-' means compression

Figures Caption

Figure 1 (a) Schematic diagram of the fabrication and growth procedure of our overgrown AlGaN; (b) Typical cross-sectional SEM image of our semi-polar (11-22) AlGaN on the non-coalesced overgrown GaN. The circle shows our semipolar AlGaN laterally grown on the non-coalesced GaN voids. Inset: a typical top-view SEM image of our overgrown AlGaN.

Figure 2 (a) XRD spectra measured in a ω/2θ scanning mode for all the samples; (b) Normalized PL spectrum of all the samples measured at room temperature.

Figure 3 (a) XRD rocking curves as a function of an azimuth angle for our overgrown (11-22) AlGaN with 37.8% Al, the as-grown GaN template, the underlying overgrown GaN and the standard AlGaN with similar Al composition for comparison; (b) FWHMs of XRD rocking curves measured along [1-100] and [11-2-3] for all the overgrown AlGaN samples as a function of Al composition; and (c) Anisotropy degree for all the overgrown AlGaN samples as a function of Al composition.

Figure 4 XRD RSM of the overgrown AlGaN sample with Al composition of 39.9% measured along the [1-100] direction (a); and along the [11-2-3] direction

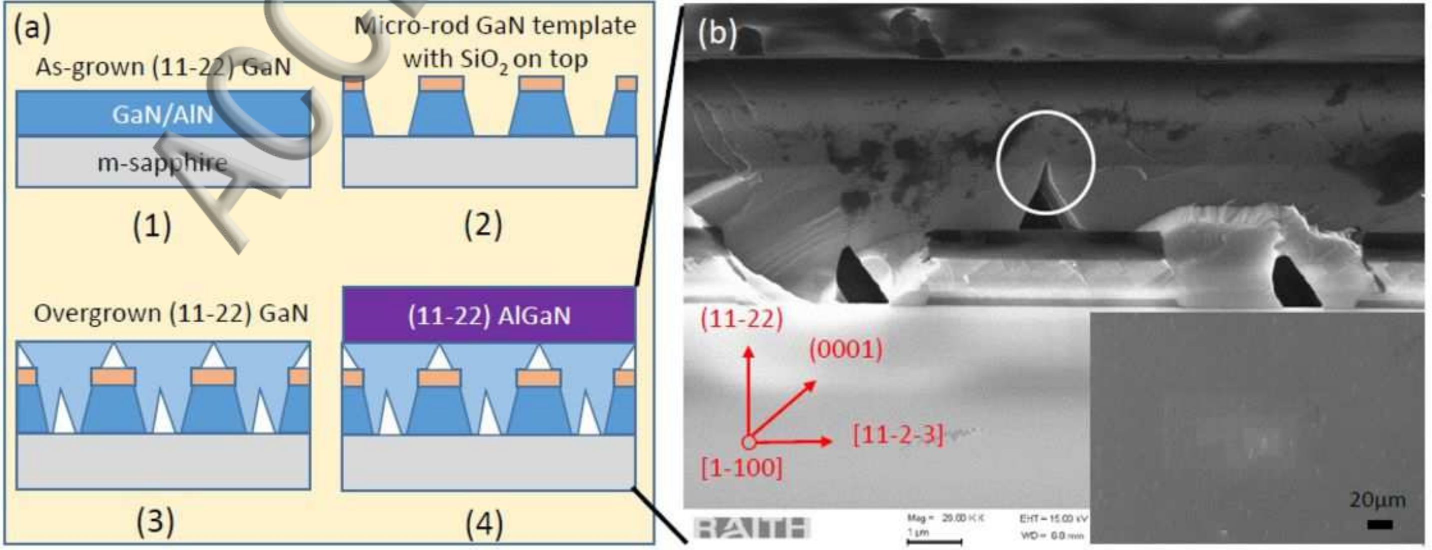
(a)
As-grown (11-22) GaN
GaN/AlN
m-sapphire
(1)
Micro-rod GaN template with SiO_2 on top
(2)
Overgrown (11-22) GaN
(3)
(11-22) AlGaN
(4)
(b)
(11-22)
(0001)
[11-2-3]
[1-100]
20μm
RAITH
Mag = 20.00 K X
1 μm
EHT = 15.00 kV
WD = 6.0 mm

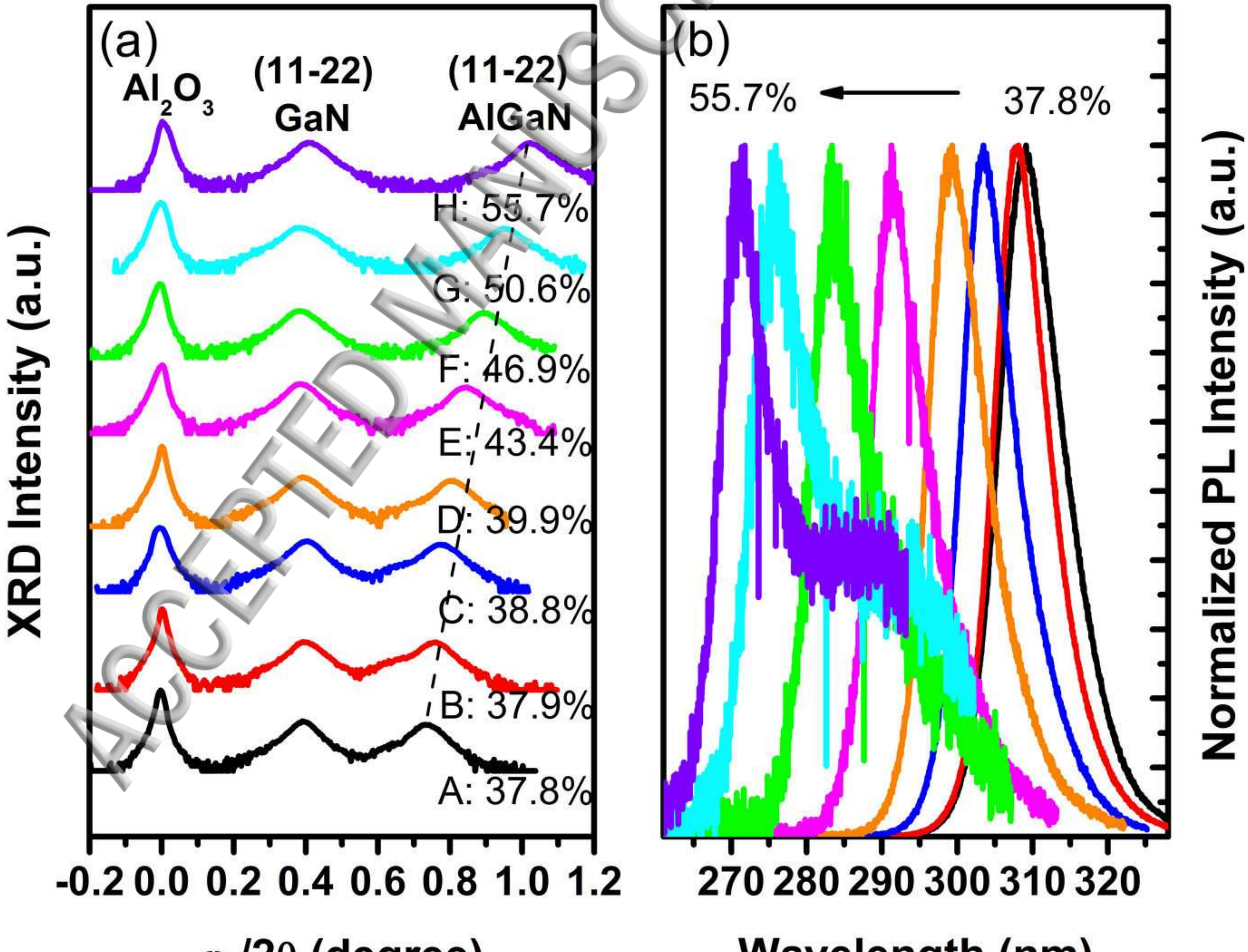
(a)
Al2O3
(11-22)
GaN
(11-22)
AlGaN
H: 55.7%
G: 50.6%
F: 46.9%
E: 43.4%
D: 39.9%
C: 38.8%
B: 37.9%
A: 37.8%
XRD Intensity (a.u.)
-0.2
0.0
0.2
0.4
0.6
0.8
1.0
1.2
ω /2θ (degree)
(b)
55.7%
37.8%
Normalized PL Intensity (a.u.)
270
280
290
300
310
320
Wavelength (nm)

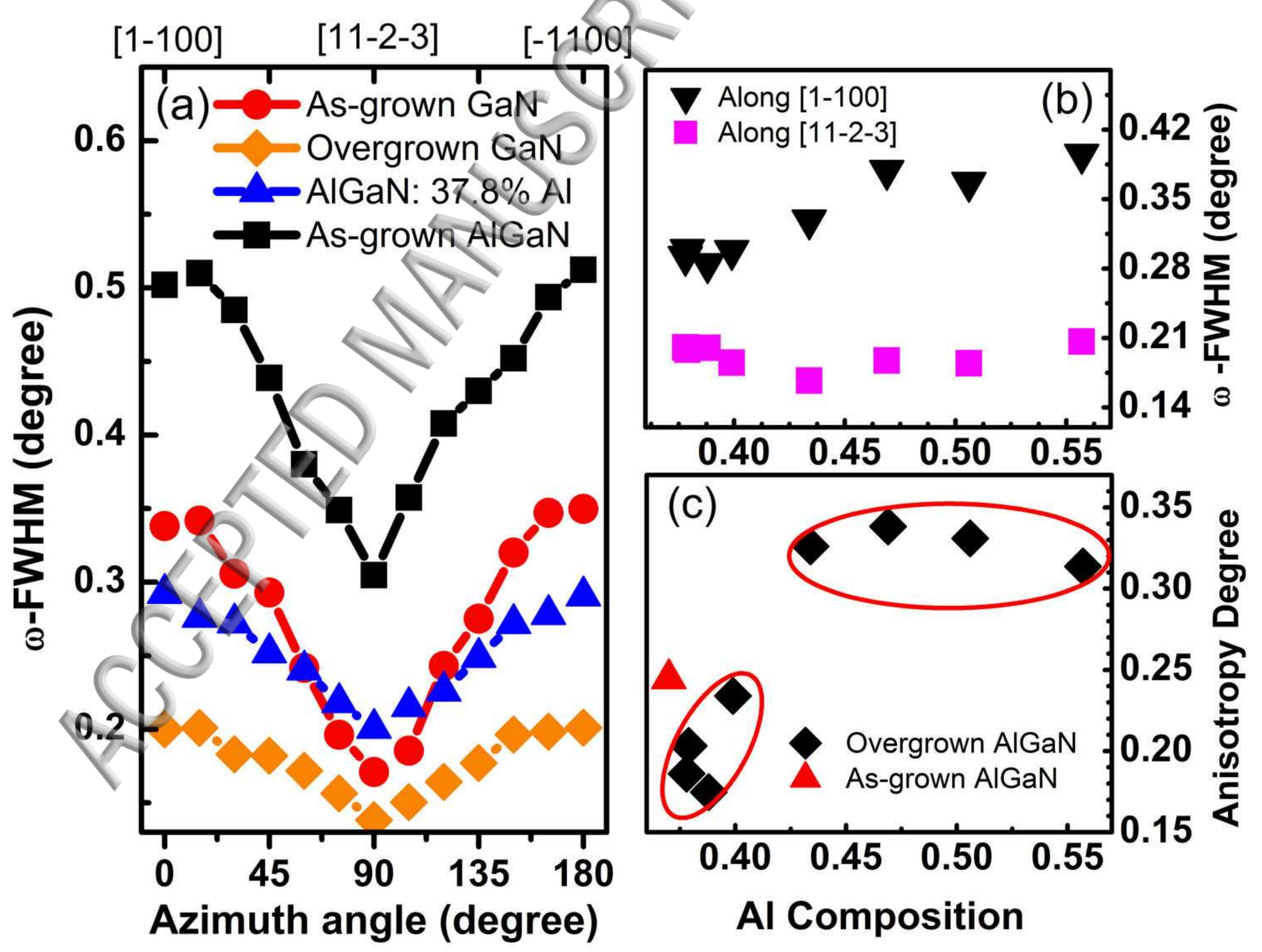
[1-100]
[11-2-3]
[-1100]
(a)
As-grown GaN
Overgrown GaN
AlGaN: 37.8% Al
As-grown AlGaN
ω-FWHM (degree)
0.2
0.3
0.4
0.5
0.6
0
45
90
135
180
Azimuth angle (degree)
(b)
Along [1-100]
Along [11-2-3]
ω -FWHM (degree)
0.14
0.21
0.28
0.35
0.42
0.40
0.45
0.50
0.55
(c)
Overgrown AlGaN
As-grown AlGaN
Anisotropy Degree
0.15
0.20
0.25
0.30
0.35
0.40
0.45
0.50
0.55
Al Composition

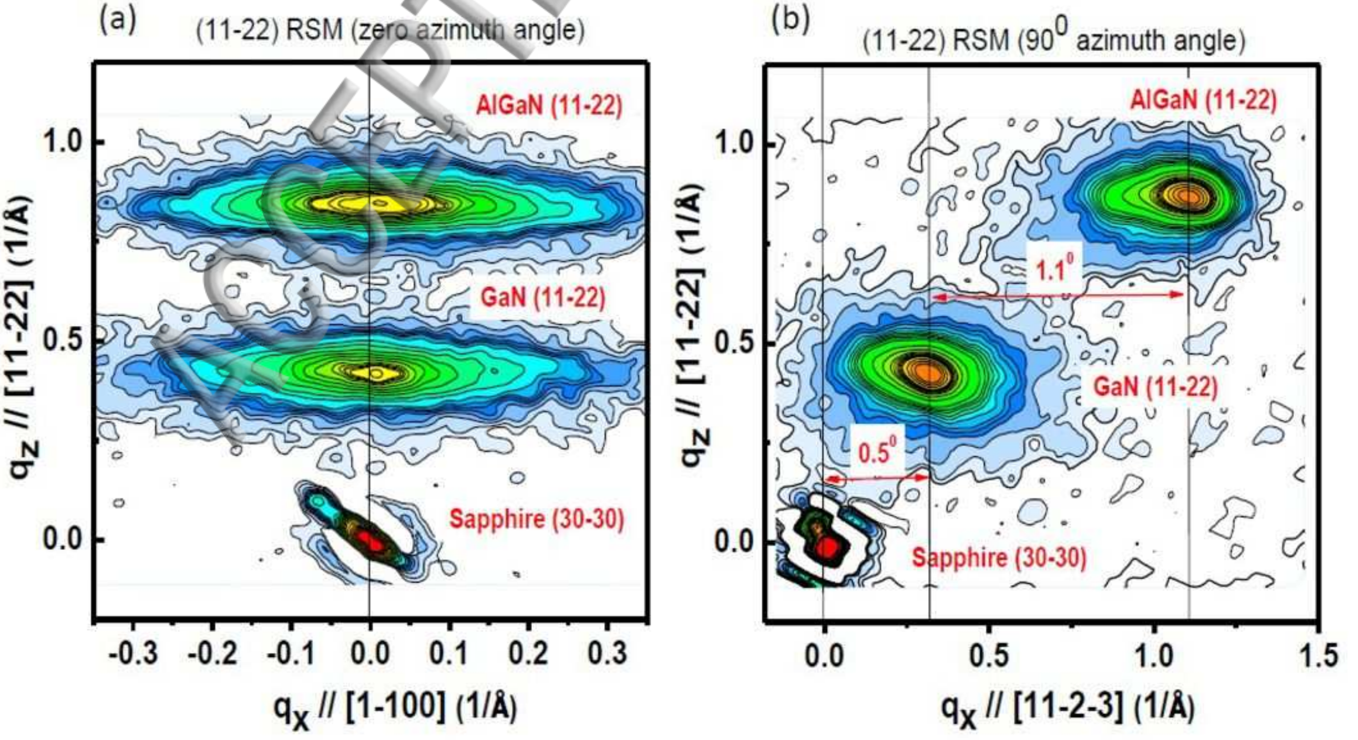
(a)
(11-22) RSM (zero azimuth angle)
AlGaN (11-22)
GaN (11-22)
Sapphire (30-30)
1.0
0.5
0.0
q_z // [11-22] (1/Å)
-0.3
-0.2
-0.1
0.0
0.1
0.2
0.3
q_x // [1-100] (1/Å)
(b)
(11-22) RSM (90^0 azimuth angle)
AlGaN (11-22)
1.1^0
GaN (11-22)
0.5^0
Sapphire (30-30)
1.0
0.5
0.0
q_z // [11-22] (1/Å)
0.0
0.5
1.0
1.5
q_x // [11-2-3] (1/Å)